moreover, the EPR spectrum of structure a would probably be rendered axial by internal motion.

2. Semioccupied Orbitals. With regard to A, little can be said about the spin-population distribution since data are only available for a single direction. The semioccupied molecular orbital (SOMO) of A presumably consits of an antibonding combination of the Ni $3d_{x^2}$ or $3d_{z^2}$ orbitals with no requirement that the resultants lie along the Ni···Ni direction. There may well be a considerable contribution to the SOMO from bridging C 2p orbitals, in view of the large ^{13}C hyperfine interaction from these nuclei.

The key to a correct description of the SOMO for species B lies in the relative signs of the ^{61}Ni tensor components, which are not established. If opposite signs are assumed, the usual method[9] yields an estimated spin population of 0.75 in *each* Ni 3d orbital. The inclusion of spin density on the ligands leads then to an unacceptably high total unpaired spin density. The alternative assumption of all signs the same is only acceptable if the Ni character is essentially 4p: Although we have no estimate for Ni $\langle r^{-3}\rangle_{4p}$, we known its value must be very small. Accordingly, even quite small ^{61}Ni hyperfine anisotropy may imply a substantial unpaired spin population in Ni $4p_z$. It would appear, then, that the anionic formulation $Ni_2(CO)_7^-$ fits the observations best. For the SOMO, we envisage an antibonding combination of two Ni $4p_z$ orbitals and a C $2p_z$ orbital. The observed small negative g shifts are consistent with a single electron in an otherwise empty set of p orbitals.

For species C, we estimate a spin population of 0.23 in each Ni 3d orbital constituent of the SOMO. Considerable spin density must reside on the ligand nuclei, therefore, although the ^{13}C hyperfine data appear to belie this. The observed hyperfine interactions for the group of four carbons may not be principal values, however. Consider the structure and molecular orbital

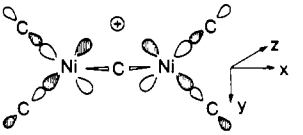

Cylindrical ^{13}C tensors of (7, −1, −1 G) placed 90° apart at the four terminal positions would be observed as four equivalent nuclei with $|a_{xx}| = 5$ G, $|a_{yy}| = 5$ G, and $|a_{zz}| = 1$ G, exactly as measured (Table I). Such ^{13}C tensors account for as much as 28% unpaired spin density.

The bridging carbons cannot contribute p_x or p_z character directly to this b_{2u} (in D_{2h}) orbital suggested for $Ni_2(CO)_6^+$. They appear to contribute a small amount of s character, and even that may be through polarization. This may account for the anomalously small hyperfine interactions of the bridging ^{13}C nuclei in this species.

Registry No. $Ni_2(CO)_8^+$, 97731-86-7; $Ni_2(CO)_7^-$, 97731-87-8; $Ni_2(CO)_6^+$, 97731-88-9; $Ni(CO)_4$, 13463-39-3.

(9) Morton, J. R.; Preston, K. F. *J. Magn. Reson.* **1978**, *30*, 577.
(10) Brown, T. L.; Sweany, R. L. *Inorg. Chem.* **1977**, *16*, 415.
(11) Brown, T. L.; Sweany, R. L. *Inorg. Chem.* **1977**, *16*, 421.

Contribution from the Max-Planck-Institut für Festkörperforschung, 7000 Stuttgart 80, Federal Republic of Germany

Metal–Metal Bonding in Transition-Element and Lanthanoid Cluster Compounds. 2

D. W. BULLETT*

Received December 5, 1984

Electronic structure calculations are reported for a number of metal-rich lanthanoid cluster halides, Gd_2Cl_3, Er_4I_5, Er_6I_7, and Er_7I_{10} (and also $NaMo_4O_6$), all of which contain trans-edge-linked (single or double) chains of lanthanoid octahedra, as well as C_2-filled cluster compounds such as $Gd_{10}C_4Cl_{18}$, $Gd_{10}C_4Cl_{17}$, and $Gd_{12}C_6I_{17}$, and the saltlike compound Gd_2NCl_3. The origin of the chemical bonding is analyzed, with particular reference to the extent of metal–metal bonding in each case. The semiconducting gap $E_g \sim 0.7$ eV calculated for Gd_2Cl_3 arises because three d-like states per Gd_4Cl_6 unit are pulled down in energy below the other d states, and these three states may be loosely interpreted as the σ and π states of the strong Gd–Gd bond shared between neighboring octahedra.

In a recent paper[1] electronic structure investigations were reported for a number of metal-rich halides of transition elements and rare-earth metals with particular regard to their metal–metal bonding content. The simplest example considered was NbI_4, in which the metal–metal bonds linking alternate Nb atoms could be clearly identified. The geometrical arrangement of atoms in NbI_4 is such that one of the metal d subbands (consisting primarily of the paired d_{z^2} bonding orbitals directed along the chain direction) is split off below the others, and a clear semiconducting energy gap of about 0.4 eV separates the highest occupied band of metal–metal-bonding states from the lowest unfilled d band. For the double-layer structure of ZrCl a composite group of d bands is pulled down in energy, without a complete energy separation from the higher d bands; the Fermi level E_F falls in a deep, but nonzero, dip in the semimetallic density of states, and no rigorous transformation is possible between the occupied d bands and localized metal–metal-bonding states involving specified d orbitals. It was also shown by a density-of-states calculation that semiconducting behavior would occur in the rather complicated Gd_2Cl_3 structure, although the origin of the calculated (and experimentally observed) 0.7-eV energy gap between occupied and empty states in this material was not clear. In the present submission we begin by analyzing the Gd_2Cl_3 band structure in more detail, to identify the origin of the semiconducting energy gap and to compare the Gd_2Cl_3 bands with those of the closely related $NaMo_4O_6$ structure. We also report calculations of the electronic structure in a number of other metal-rich rare-earth-metal halides, assessing the extent of metal–metal bonding in each case: Er_4I_5, Er_7I_{10}, $Gd_{10}C_4Cl_{18}$, $Gd_{10}C_4Cl_{17}$, $Gd_{12}C_6I_{17}$, and the saltlike Gd_2NCl_3. All the computations follow the method defined earlier,[1] using a basis set of numerical orbitals calculated for neutral atoms—the s, p, and d valence-level orbitals on metal (M) sites, and valence s and p atomic orbitals on ligand (X) sites (as well as Na or C positions where applicable). All matrix elements are calculated by direct numerical integration in the two-center approximation; there are no empirical parameters in this approach. The crystal potential is constructed by overlapping the neutral-atom charge densities of the constituents, with a local-density

* Address corresondence to the School of Physics, University of Bath, Bath BA2 7AY, England.

(1) D. W. Bullett, *Inorg. Chem.*, **19**, 1780 (1980). A more complete account of the computational procedure used to derive these results may be found in D. W. Bullett, *Solid State Phys.*, **35**, 129 (1980).

0020-1669/85/1324-3319$01.50/0

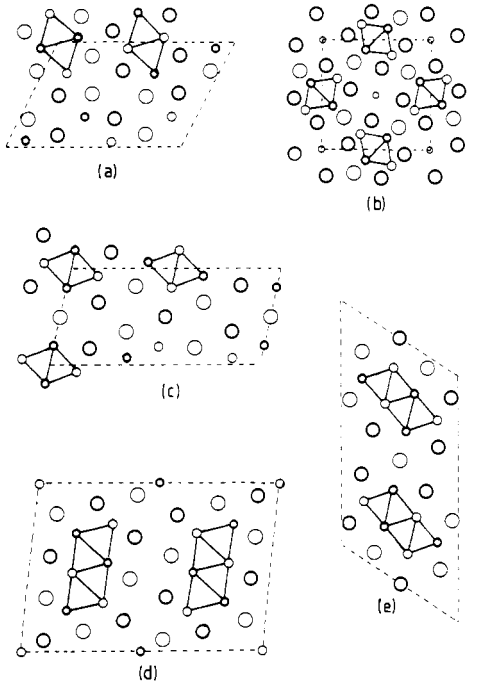

Figure 1. Crystal structures derived from condensation of M_6X_8 and M_6X_{12} clusters into trans-edge-linked chains (a) Gd_2Cl_3, (b) $NaMo_4O_6$, and (c) Er_4I_5 and the double chains of M_6X_{12} clusters (d) Er_7I_{10} and (e) Er_6I_7 (after Simon[4]). All structures are projected down the chain axis. Smaller circles denote metal atoms, and larger circles denote the surrounding ligands; the planes of the light and heavy circles are separated by half the repeat distance along the chain.

approximation for exchange and correlation. Self-consistency is included only to the extent that the metal atom d level is required to be consistent with that of a neutral atom with the same d orbital occupation.

The crystal structures of metal-rich lanthanoid halides and chalcogenides are characterized by the occurrence of isolated or connected metal clusters.[2-5] In the case of Gd_2Cl_3[6,7] (and similarly Gd_2Br_3, Tb_2Cl_3, and many other M_2X_3 lanthanoid halides[8]), metal octahedra share opposite edges to form infinite linear chains (Figure 1). Chlorine atoms occupy positions above the triangular faces of the octahedra; some additional Cl atoms are located in bridge sites between the chains of octahedra. Apart from these extra bridging halogens, the Gd_2Cl_3 structure may be viewed as a linear condensation of M_6X_8 octahedral clusters[9] into single chains, analogous to the double chains of edge-sharing M_6X_8 clusters in ScCl and GdCl.[11] Close relatives to these M_6X_8 chain compounds are the structures containing trans-edge-linked chains of M_6X_{12} clusters, such as $NaMo_4O_6$[12] and related molybdates,[13,14]

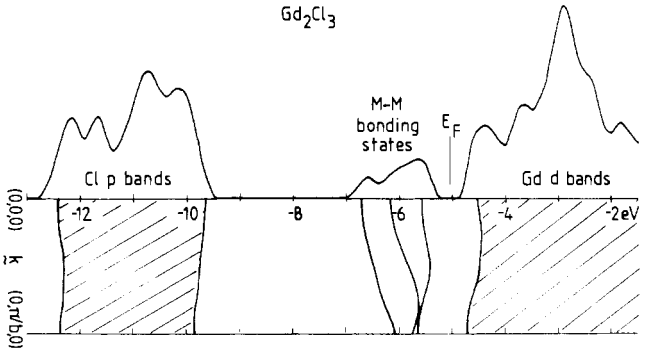

Figure 2. Calculated density of states in Gd_2Cl_3, with band dispersion, along the chain axis, of the four lowest Gd d bands and the lowest and highest Cl p bands. The Fermi level E_F falls in the gap above the three lowest Gd metal–metal-bonding bands. In this and the following figures the calculated density-of-states histograms have been smoothed by a Gaussian of standard deviation 0.1 eV.

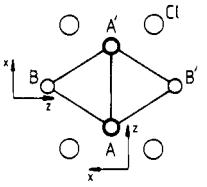

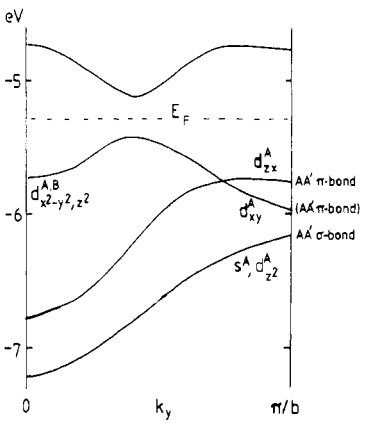

Figure 3. Dispersion of the four lowest d bands calculated for a single $[(Gd_4Cl_4)^{2+}]_\infty$ chain. The metal–metal-bonding bands are labeled according to the local coordinate system shown, with $\hat{y}$ pointing along the chain axis and $\hat{z}$ pointing into the center of the chain from Gd atoms of type A or B, respectively.

Sc_5Cl_8,[15,16] Sc_7Cl_{12},[17,18] and Er_4I_5,[19] and the double-chain M_6X_{12} cluster compounds such as Er_6I_7[20] and Er_7I_{10}.[19] Simon[4] has provided a very clear and comprehensive review of the structural chemistry of most of the known condensed metal cluster halides.

Gd_2Cl_3

Figure 2 illustrates the calculated dispersion of electronic states as a function of their rate of change of phase (k_2) along the chain

(2) A. Simon, *Chem. Unserer Zeit*, **10**, 1 (1976).
(3) H. F. Franzen, *Prog. Solid State Chem.*, **12**, 1 (1978).
(4) A. Simon, *Angew. Chem.* **93**, 23 (1981); *Angew. Chem., Int. Ed. Engl.*, **20**, 1 (1981).
(5) J. D. Corbett, *J. Solid State Chem.*, **37**, 335 (1981).
(6) J. E. Mee and J. D. Corbett, *Inorg. Chem.*, **4**, 88 (1965).
(7) D. A. Lokken and J. D. Corbett, *Inorg. Chem.*, **12**, 556 (1973).
(8) A. Simon, N. Holzer, and Hj. Mattausch, *Z. Anorg. Allg. Chem.*, **456**, 207 (1979).
(9) For calculations of the electronic structure in the "Chevrel phase" compounds, in which the Mo_6X_8 cluster is preserved intact as the fundamental structural unit, see for example: O. K. Andersen, W. Klose, and H. Nohl, *Phys. Rev. B: Solid State* **17**, 1209 (1978); H. Nohl, W. Klose, and O. K. Andersen in "Superconductivity in Ternary Compounds", Ø. Fisher and M. B. Maple, Eds.; Springer Verlag, West Berlin, 1982; D. W. Bullett, *Phys. Rev. Lett.*, **39**, 664 (1977); T. Hughbanks and R. Hoffmann, *J. Am. Chem. Soc.*, **105**, 1150 (1983).
(10) K. R. Poeppelmeier and J. D. Corbett, *Inorg. Chem.*, **16**, 1107 (1977).
(11) A. Simon, Hj. Mattausch, and N. Holzer, *Angew. Chem.*, **88**, 685 (1976); *Angew. Chem., Int. Ed. Engl.*, **15**, 624 (1976).
(12) C. C. Torardi and R. E. McCarley, *J. Am. Chem. Soc.*, **101**, 3963 (1979).
(13) C. C. Torardi and R. E. McCarley, *J. Solid State Chem.* **37**, 393 (1981).
(14) R. E. McCarley, "Inorganic Chemistry: Toward the 21st Century", M. H. Chisholm, Ed., American Chemical Society, Washington, DC, 1983, ACS Symp. Ser. No. 211, p 237.
(15) K. R. Poeppelmeier and J. D. Corbett, *J. Am.* Chem. *Soc.*, **100**, 5039 (1978).
(16) Hj. Mattausch, A. Simon, and R. Eger, *Rev. Chim. Miner.* **17**, 516 (1980).
(17) J. D. Corbett, R. L. Daake, K. R. Poeppelmeier, and D. H. Guthrie, *J. Am. Chem. Soc.*, **100**, 652 (1978).
(18) J. D. Corbett, K. R. Poeppelmeier, and R. L. Daake, *Z. Anorg. Allg. Chem.*, **491**, 51 (1982).
(19) K. Berroth and A. Simon, *J. Less-Common Met.*, **76**, 41 (1980).
(20) K. Berroth, Hj. Mattausch, and A. Simon, *Z. Naturforsch, B: Anorg. Chem., Org. Chem.*, **35B**, 626 (1980).

Table I. Orbital Decompositions of the Lowest Gd d Bands in the Isolated $[Gd_4Cl_4]_\infty$ Chain Taken from the Gd_2Cl_3 Structure for the Two Wave Vectors $k_y = 0$ and $k_y = \pi/b$[a]

energy, eV	% on Gd(A) orbitals									% on Gd(B) orbitals								
	s	x	y	z	xy	yz	zx	x^2-y^2	z^2	s	x	y	z	xy	yz	zx	x^2-y^2	z^2
								$k_y = 0$										
−4.7	2			2				26	24	20			6					14
−5.7	10			2			2	16	18	6			2				16	24
−6.8		6					18			46							26	
−7.2	28			6				2	10	40							14	
								$k_y = \pi/b$										
−4.8							2	10	6					86				
−5.8		4					38		2			2			52			
−6.0			8		50					12						2		24
−6.2	28			4				2	32			2			28			

[a] For definitions of the atomic labels and local coordinate systems, see Figure 3.

direction and the corresponding density of electron states as a function of energy. The electron count in Gd_2Cl_3 is such as to exactly fill the three lowest d bands; thus, the highest filled state lies at −5.4 eV, and the lowest unfilled state occurs at −4.7 eV. This calculated semiconducting energy gap E_g of 0.7 eV is much in line with experimental measurements on Gd_2Cl_3: Bauhofer and Simon[21] estimated $E_g = 0.85$ eV from the temperature dependence of electrical resistivity, and the photoelectron spectra[22] also suggested a semiconducting gap of approximately 1 eV. To avoid a confusion of spaghetti in Figure 2, only the uppermost of the 18 Cl p bands and the lowest of the Gd d conduction bands is shown. The individual bands are strongly one-dimensional, with bandwidths of typically 0.5 eV along the chain direction compared to ~0.1 eV inthe perpendicular directions. The photoelectron spectra[22] confirm that this picture of the density of occupied states is essentially correct: in the experimental data the highest valence-band peak (attributed to occupied Gd 5d states) is centered about 1.3 eV below the Fermi level E_F and has a width ~1.2 eV, while the next more strongly bound peak (attributed to Cl 3p states) is centered 7.4 eV below E_F, with a width ~2–3 eV. The Gd 4f orbitals have not been included explicitly in the band structure calculation; from the initial atomic calculation for a neutral $4f^7$ configuration they should form localized levels at −12.2 eV, i.e. just below the calculated Cl 3p band, and such states have been detected in photoelectron spectra.[22]

For a chemical interpretation of the origin of the semiconducting band gap, it is convenient to look at the lowest d bands for a single $(Gd_4Cl_4)_\infty$ chain, i.e. an isolated chain from the Gd_2Cl_3 structure, neglecting the effects of bridging Cl atoms. We choose a local coordinate system such that $\hat{y}$ lies along the chain direction and $\hat{z}$ points into the center of the chain from each Gd atom. The four lowest d bands (Figure 3) show the same behavior as those for the full structure, albeit with a reduced (0.4 eV) energy gap between bands 3 and 4. Of the three lowest d bands, two are symmetric with respect to reflection in the plane containing the chain axis and the shared edges AA′ of the octahedra, and the third is antisymmetric. Table I shows the detailed orbital decomposition for phases $k_y = 0$ and $k_y = \pi/b$. The Gd octahedra making up the chain are considerably distorted: Gd–Gd separations are AA′ = 3.37 Å along the shared edge, and AB = 3.73, 3.79 Å and AA = BB = 3.90 Å along the chain axis. From Table I we can see why this distortion takes place. Loosely interpretated, the lowest d band corresponds to the strong σ bond (s^A, $d^A_{z^2}$ orbitals) between atoms A and A′, and the next two bands are the AA′ π bonds—d^A_{zx} for the state of odd symmetry with respect to the AA′y plane, representing the π bond in the plane perpendicular to the chain direction, and d^A_{xy} representing the π bond within the AA′y plane. The energy of this third band naturally depends rather sensitively on the rate of change of phase along the chain, and the semiconducting gap really results from hybridization of the AA′ π-bonding state in the AA′y plane with the ($d^A_{x^2-y^2}$) band, which, for k values close to $k_y = 0$, tends to bond atoms AA and BB along the chain direction. Of course a full explanation of the electronic structure would be very complicated—the role of the ligands and type B Gd atoms cannot really be neglected. However the simplest interpretation does seem to approximate the true picture: the octahedral chains in Gd_2Cl_3 distort so that the three occupied d bands are split off below the others, the distortion involves a strengthening of the AA′ bond along the shared edges, and the occupied states may be associated with one σ and two π bonds along this edge.

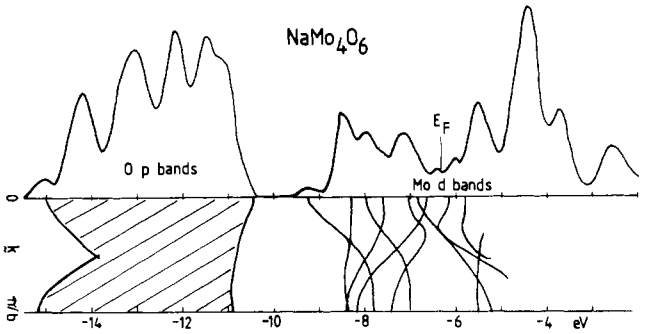

Figure 4. Calculated bands and density of states for electrons in a single chain $[Mo_4O_6]_\infty$ taken from the $NaMo_4O_6$ structure (see Figure 1). The marked position of E_F corresponds to the d-band occupancy (13 e/formula unit) in $NaMo_4O_6$.

$NaMo_4O_6$

The strong distortions in the Gd_2Cl_3 system are a consequence of the low formal d occupancy of only 6 electrons per M_4 unit along the chain. In a one-dimensional molybdate such as $NaMo_4O_6$, we have 13 electrons per M_4 unit, enough to occupy virtually all M–M bonding combinations of d orbitals within the octahedral chain structure. Hence there is much less variation between the shared trans-edge distance AA′ (2.75 Å), the other octahedral edges AB (2.78 Å), and the intrachain repeat distance AA = BB = 2.86 Å. Figure 4 illustrates the calculated d bands and density of states for a single $[Mo_4O_6]_\infty$ chain taken from the $NaMo_4O_6$ structure. The sequence of bands is different from that for Gd_2Cl_3 because of the different disposition of ligands. The molybdate chains[12-14] occur by condensation of M_6X_{12} (as opposed to M_6X_8) clusters, with ligands above the metal octahedron edges (as opposed to triangular faces). On each M site, the energies of two d orbitals are pushed up by interaction with the four of five surrounding ligands, leaving the three low-lying orbitals of the t_{2g} set. From these, the structural arrangement of the four M atoms per unit cell of the chain induces six bonding and six antibonding bands, with a slight overlap of the two groups near $k = 0$. At a formal electron count of $d^{3.25}$ there is apparently no energy-favorable distortion that can induce a semiconducting gap analogous to that in Gd_2Cl_3.

Metal–metal bonding in the $NaMo_4O_6$ system has been analyzed in detail by Hughbanks and Hoffmann[23] using the extended

(21) W. Bauhofer and A. Simon, *Z. Naturforsch, A: Phys., Phys. Chem., Kosmophys.*, **37A**, 568 (1982).
(22) G. Ebbinghaus, A. Simon, and A. Griffith, *Z. Naturforsch, A: Phys., Phys. Chem., Kosmophys.*, **37A**, 564 (1982).

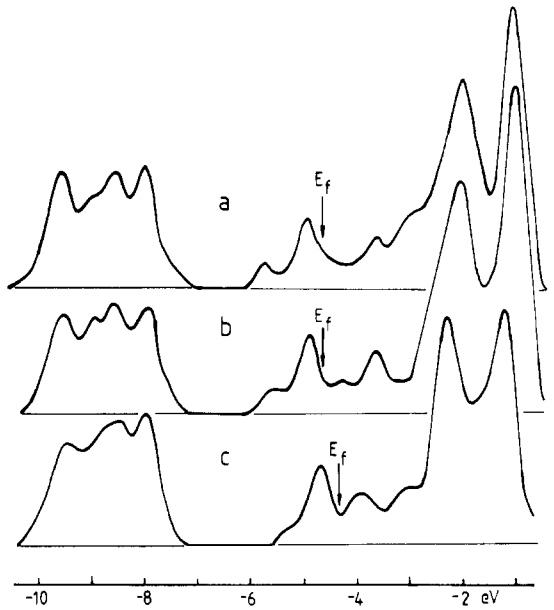

Figure 5. Densities of states calculated for (a) a single $[(Er_4I_6)^-]_\infty$ chain taken from the Er_4I_5 structure, (b) the full three-dimensional Er_4I_5 crystal, and (c) the double-chain structure of Er_6I_7 and Er_7I_{10} (see Figure 1).

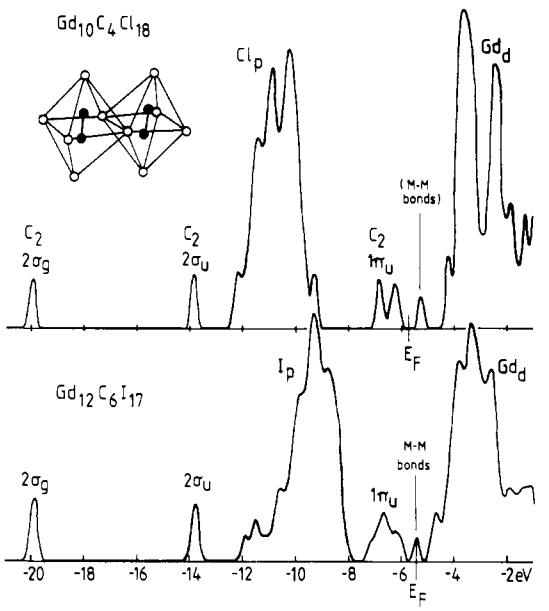

Figure 6. Calculated distributions of electron states in the C_2-filled cluster compounds $Gd_{10}C_4Cl_{18}$ and $Gd_{12}C_6I_{17}$. In $Gd_{10}C_4Cl_{18}$ chlorine atoms bridge each edge of the Gd_{10} double octahedron shown in the inset. Highest occupied states are derived from the antibonding π states of the C_2 dimers; lowest unoccupied states (partially filled in the case of $Gd_{10}C_4Cl_{17}$ and $Gd_{12}C_6I_{17}$) are the Gd metal–metal-bonding states.

Hückel parameterization scheme. The band shapes arising from the present nonempirical calculations are in fact remarkably similar to the extended Hückel results, so that no further analysis of the electronic structure is necessary here. One rather obvious difference is that the occupied d bandwidth in Figure 4 (3.0 eV) is much larger than in the semiempirical calculations (1.8 eV). Part of this discrepancy may originate in the much smaller Mo 4d–O 2p energy difference (3.7 eV) of the extended Hückel parameters; in the present calculations we find that the self-consistent d-orbital occupation on Mo atoms is $d^{4.2}$, corresponding to an atomic d level at −6.5 eV compared to the oxygen 2p level at −11.4 eV. Our oxygen p bands themselves span the energy range −10.4 to −15.0 eV.

Metal-Rich Erbium Iodides: Er_4I_5, Er_6I_7, and Er_7I_{10}

Metal-rich erbium iodides have recently been shown to provide several new examples of structures based on linear condensations of M_6X_{12} clusters. Er_4I_5 (Figure 1) contains single chains of trans-edge-sharing Er_6 octahedra,[19] like those in $NaMo_4O_6$. In Er_6I_7 the M_6X_{12} clusters condense into double chains of trans-edge-sharing metal octahedra;[20] similar double chains occur in Er_7I_{10}, with the addition now of isolated Er atoms in sites octehedrally coordinated by iodine atoms.[19] For both the single and double chains the calculated densities of states (Figure 5) shows a peak of predominantly metal–metal-bonding states developing at the bottom of the d band, with the Fermi energy E_F lying in the valley at an energy just above this occupied peak. The marked positions of E_F are those appropriate to the electron numbers in Er_4I_5 and Er_7I_{10}, respectively, assuming the f-electron configuration is $4f^{11}$.

C_2-Filled M_6X_{12} Clusters: $Gd_{10}C_4Cl_{18}$, $Gd_{10}C_4Cl_{17}$, and $Gd_{12}C_6I_{17}$

Several novel lanthanoid cluster compounds containing interstitial C_2 units have recently been prepared.[24] $Gd_{10}C_4Cl_{18}$ and $Gd_{10}C_4Cl_{17}$ each contain a metal framework formed by edge sharing of pairs of Gd_6 octahedra.[25] A C_2 dimer (with C–C separation of 1.47 Å) sits at the the center of each octahedron. Cl atoms bridge all available edges of the double octahedron. In the former compound these $Gd_{10}C_4Cl_{18}$ clusters pack as quasi-molecular units; in the latter compound the clusters are linked via shared Cl atoms. In the case of $Gd_{12}C_6I_{17}$,[26] the Gd_6I_{12} cluster condensation goes much further, into zigzag chains of Gd_6 octahedra linked via cis and trans edges, but once again C_2 dimers occupy the center of each octahedron.

Actually the degree of metal–metal bonding is rather slight in these compounds, especially in the case of $Gd_{10}C_4Cl_{18}$, where an appropriate way of looking at the structure is as a salt containing Cl^- and $(C_2)^{6-}$ anions and Gd^{3+} cations.[25] The calculated distributions of electron states (Figure 6) demonstrates the validity of this picture.[27] Formally, the occupied states in $Gd_{10}C_4Cl_{18}$ are (in approximate order of increasing energy) the C_2 bonding and antibonding s-like states $2\sigma_g$ and $2\sigma_u$, the bonding p-like state $3\sigma_g$, and the bonding and antibonding π states $1\pi_g$ and $1\pi_u$, respectively, together with the filled shells of Cl 3p states. The $3\sigma_g$ and $1\pi_g$ states cannot be separately identified in the calculated spectrum, because their energies overlap the Cl p states. The unoccupied $3\sigma_u$ orbitals provide the formal stabilization energy that binds the two atoms of the C_2 dimer together, at a separation typical of C–C single-bond distances. In reality, of course, the C_2 group with formal charge −6 is stable only because of strong hybridization with the d orbitals of the surrounding Gd anions. For example, the orbital composition of the "$1\pi_u$ states" is in fact 50% Gd, 5% Cl, and only 45% C_2, and summing the Mulliken orbital populations over all occupied states gives charge distributions of approximately $Gd^{1.6}$, $Cl^{0.7-}$, $(C_2)^{2.0-}$ on the three types of ions.

The lowest unoccupied orbital in $Gd_{10}C_4Cl_{18}$ is a metal–metal-bonding state, split off by about 1 eV from the main Gd d bands (with which the unoccupied $3\sigma_u$ state hybridizes). In the more electron-rich compounds $Gd_{10}C_4Cl_{17}$ and $Gd_{10}C_4Cl_{16}$, this M–M bonding band is partially, or fully, occupied and the Gd–Gd edge linking the two octahedra shortens accordingly, from 3.21 Å in $Gd_{10}C_4Cl_{18}$ to 3.12 Å in $Gd_{10}C_4Cl_{17}$.

Very similar effects can be seen in the calculated spectrum for $Gd_{12}C_6I_{17}$. The Fermi level E_F again falls in the middle of the M–M bonding band, which occurs above the C_2 π^*-like states but

(23) T. Hughbanks and R. Hoffmann, *J. Am. Chem. Soc.*, **105**, 3528 (1983).
(24) A. Simon, E. Warkentin, and R. Masse, *Angew. Chem.*, **93**, 1071 (1981); *Angew. Chem., Int. Ed. Engl.*, **20**, 1013 (1981).
(25) E. Warkentin, R. Masse, and A. Simon, *Z. Anorg. Allg. Chem.*, *491*, 323 (1982).
(26) A. Simon and E. Warkentin, *Z. Anorg. Allg. Chem.*, *497*, 79 (1983).
(27) A similar description of the electron states in the $Gd_{10}C_4Cl_{18}$ cluster has been found from a self-consistent muffin-tin-orbital study: S. Satpathy and O. K. Andersen, to be submitted for publication.

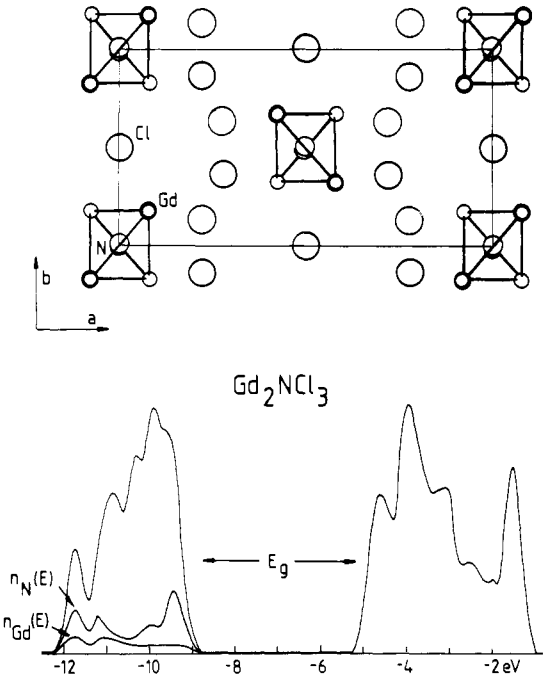

Figure 7. Gd_2NCl_3 structure[28] and corresponding energy distribution of electron states, showing the saltlike division into filled-anion-derived and empty-cation-derived bands.

below the main group of Gd d bands. Calculated ionic charges in this case are $Gd^{1.2}$, $I^{0.5-}$, and $(C_2)^{1.7-}$.

Gd_2NCl_3

Finally we consider the electronic structure of the truly saltlike rare-earth-metal nitride chloride Gd_2NCl_3. This compound has very recently been prepared, by reacting $GdCl_3$ with Gd and nitrogen or with GdN, and structurally analyzed by Schwanitz-Schüller and Simon.[28] It is possible to view the Gd_2NCl_3 structure (Figure 7) as a derivative of Gd_2Cl_3. The linear chains of trans-edge-sharing Gd octahedra have been stretched into chains of Gd tetrahedra, with a nitrogen atom at each tetrahedron center. Gd–Gd distances along the shared edges of the tetrahedra are 3.35 Å (as in the equivalent edges of Gd_2Cl_3), compared to 3.83–3.97 Å along the other edges; the average Gd–Gd distance of 3.78 Å is only slightly larger than that in Gd_2Cl_3 (3.72 Å).[8] Whereas the dimer bonding of the C_2 groups in the compounds of the previous section was provided by leaving the antibonding $3\sigma_u$ states unoccupied, in the nitride chlorides the corresponding states of the more electronegative nitrogen fall below the Fermi level: the N_2 dimer is unbonded and separates into two, formally filled-shell, N^{3-} units. Thus it is probably more informative to regard Gd_2NCl_3 as a conventional ionic salt, $(Gd^{3+})_2N^{3-}(Cl^-)_3$, containing a close packing of filled-shell spherical ions and with no spare electrons for metal–metal bonding.

Electronic structure calculations for a single one-dimensional chain of Gd_2NCl_3 confirm that this saltlike picture is qualitatively correct. The density of states is that of a wide-gap insulator, with no clearly identifiable occupied metal–metal-bonding states. Chlorine and nitrogen orbitals form the dominant components of the narrow valence bands, in the energy range −11.9 to −9.1 eV, while a gap of 4.1 eV separates the highest occupied anion states from the lowest Gd d conduction states. However, metal d-orbitals do contribute substantially to the stabilization of the nitrogen ions, and Gd–N hybridization is particularly evident at the bottom of the valence band: a Mulliken population analysis attributes 0.9 e to metal d orbitals (and 0.1 e to metal sp orbitals), giving final ionic charge distributions of +2.0 on Gd, −1.8 on N, and −0.7 on Cl. Intearctions between the Gd d orbitals must be responsible, both directly and indirectly through hybridization with the nitrogen p orbitals, for the surprisingly short Gd–Gd distance on the shared edges of the tetrahedra.

Conclusion

Electronic structure calculations have been used to examine the bonding character, and particularly the extent of metal–metal bonding, in a number of condensed cluster compounds of transition elements and rare-earth metals. The computational approach is undoubtedly crude but is probably the best available at present for such complex crystal structures. Metal–metal bonding has been shown to be strong in Gd_2Cl_3, where the three low-energy d bands per unit cell of the chain structure may be loosely interpreted as the σ- and two π-bonding states along the shared trans edges of adjacent Gd_6 octahedra. The compounds $NaMo_4O_6$, Er_4I_5, Er_6I_7, and Er_7I_{10} adopt crystal structures such that the Fermi levels E_F falls in a dip in the electron density of states, above occupied peaks of states containing bonding combinations of metal d orbitals; with no energy gap between occupied and empty states it is not possible to interpret these occupied states in a localized, chemical terminology of metal–metal bonds. The results for the C_2-filled cluster compounds $Gd_{10}C_4Cl_{18}$, $Gd_{10}C_4Cl_{17}$, and $Gd_{12}C_6I_{17}$ fall much more easily into standard chemical bonding language, with occupied molecular orbitals or crystal energy bands, which may be clearly described by labels such as "C_2 $1\pi_u$", although ~50% of the molecular orbital may actually be contributed by Gd basis functions. Formally the lowest of the Gd d bands is a metal–metal-bonding state related to the shared edge of the Gd octahedra, occupied in $Gd_{10}C_4Cl_{16}$, partially occupied in $Gd_{10}C_4Cl_{17}$ or $Gd_{12}C_6I_{17}$, and empty in $Gd_{10}C_4Cl_{18}$. Finally we considered Gd_2NCl_3, in which formal metal–metal bonding is absent. The calculated density of states for this compound is that of a conventional salt, with an energy gap of 4.1 eV separating the "anion valence band" from the "cation conduction band" and no sign of distinct metal–metal-bonding orbitals in the spectrum. However it is only the strong hybridization with the surrounding Gd d states that stabilizes the formal N^{3-} ionic configuration in this compound: a Mulliken population analysis (which must as always be treated with due caution) assigns almost one valence-band electron to the d orbitals of each Gd atom.

Acknowledgment. It is a pleasure to thank Professor O. K. Andersen and A. Simon for useful discussions at the Max-Planck-Institut für Festkörperforschung.

Registry No. Gd_2Cl_3, 12506-69-3; Er_4I_5, 76559-13-2; Er_6I_7, 74434-11-0; Er_7I_{10}, 76559-14-3; $NaMo_4O_6$, 71251-76-8; $Gd_{10}C_4Cl_{18}$, 84989-58-2; $Gd_{10}C_4Cl_{17}$, 85248-21-1; $Gd_{12}C_6I_{17}$, 96826-77-6; Gd_2NCl_3, 97806-79-6.

(28) U. Schanitz-Schüller and A. Simon, to be submitted for publication.